



UNIVERSITY OF LEEDS

This is a repository copy of *Burning Properties and Flame Propagation of Varying Size Pulverised Rice Husks*.

White Rose Research Online URL for this paper:

<http://eprints.whiterose.ac.uk/160498/>

Version: Accepted Version

Proceedings Paper:

Saeed, MA, Andrews, GE orcid.org/0000-0002-8398-1363, Phylaktou, HN et al. (1 more author) (2018) Burning Properties and Flame Propagation of Varying Size Pulverised Rice Husks. In: Proceedings of the 12th International Symposium on Hazards, Prevention and Mitigation of Industrial Explosions (ISHPMIE 2018). XII ISHPMIE, 12-17 Aug 2018, Kansas City, MO, USA. ISHPMIE .

This conference paper is protected by copyright. This is an author produced version of a conference paper presented at the 12th International Symposium on Hazards, Prevention and Mitigation of Industrial Explosions (ISHPMIE 2018). Uploaded in accordance with the publisher's self-archiving policy.

Reuse

Items deposited in White Rose Research Online are protected by copyright, with all rights reserved unless indicated otherwise. They may be downloaded and/or printed for private study, or other acts as permitted by national copyright laws. The publisher or other rights holders may allow further reproduction and re-use of the full text version. This is indicated by the licence information on the White Rose Research Online record for the item.

Takedown

If you consider content in White Rose Research Online to be in breach of UK law, please notify us by emailing eprints@whiterose.ac.uk including the URL of the record and the reason for the withdrawal request.



Kansas City, MO August 12-17, 2018

Proceedings of the 12th International Symposium on Hazards, Prevention and Mitigation of Industrial Explosions – XII ISHPMIE Kansas City, USA - August 12-17, 2018

Burning Properties and Flame Propagation of Varying Size Pulverised Rice Husks

Muhammad Azam Saeed^a, Gordon E. Andrews^b, Herodotus N. Phylaktou^b & Bernard M. Gibbs^b

E-mail: azamsaeed86@hotmail.com / profgeandrews@hotmail.com

^a Department of Chemical and Polymer Engineering, University of Engineering and Technology, Lahore (Faisalabad Campus), Pakistan

^b School of Chemical and Process Engineering, University of Leeds, LS2 9JT, Leeds, United Kingdom

Abstract

Flame propagation in different size fractions of a rice husk (RH) crop residues were investigated using an ISO 1 m³ dust explosion vessel. This was modified to operate with coarse biomass and for the determination of flame speeds. The flame speed, burning velocity and K_{st} were found to be greater for the finer fractions compared to the coarser sizes. The MEC were measured at 0.27 equivalence ratio (ϕ) for the finest fraction to 1.4 ϕ for the coarser fraction. The most reactive concentration was measured at lower ϕ for fine particles and higher ϕ for coarse particles. The maximum K_{st} for the fine particles was 83 bar m/s and 33 bar m/s for the coarse particles. The size distribution of coarse rice husk particles always has a fine fraction and the flame propagation occurs first in the fine particles, with the coarse particles burning in the hot products of combustion of the fine particles. The fine particle fraction in a coarse mixture has to be flammable and as there is a low proportion of the mixture in the fine fraction, the overall concentration of particles has to increase for the concentration of fines to be flammable. This resulted in the observed lean flammability limit that was richer than stoichiometric for coarse size mixtures.

Keywords: Dust Explosions, Flame speed, Pulverised Biomass, MEC.

1. Introduction

Renewable biomass food crop residues are a viable and low cost fuel option for power generation plants. For an agricultural country like Pakistan this locally accessible fuel source can be used as a substitute for coal for a more environmental friendly, distributed electricity grid using smaller biomass power generation plants. Pakistan is a country with almost 2/3rd of

its population involved in the agricultural sector, which accounts for 21% of GDP (Amjid et al., 2011) and 20 % of exports (Dorosh and Thurlow, 2015). The agricultural sector generates large amount of surplus residues that can be used for rural energy generation, including the generation of electricity. These dispersed agricultural biomass residues are best utilized in dispersed small electric power generators, within easy travelling distance of local farms. The only investment needed is for the collection of the waste agricultural residues and transport to a nearby power plant. There are four major crop residues in the country that have the potential to fulfil more than 50% of Pakistan's electricity demand based on the 2014 crop production and energy use statistics (Saeed et al., 2015b).

Rice is one of the major crops in Pakistan each year. According to Pakistan's federal committee on agriculture (FCA), a target of 7 million tons production of milled rice was set for the year 2015 due to sufficient water availability and normal weather condition (Asia-Rice-News, 2015). US department of agriculture (USDA) estimated the rice production in Pakistan for 2013-2014 (November-October) to be 6.7 million tons and that production raised to 6.9 million tons for 2014-2015. However this rise of 3% was not confirmed by 'National Space Agency of Pakistan (SUPARCO) and United Nation's food and agricultural organization (Asia-Rice-News, 2015). The production of milled rice for last five years is shown in Fig. 1. This shows that there was an increase of production each year except 2012 when the crops were damaged by floods. Rice husks as a waste product of the rice crop together with the plant stems are a large biomass resource for Pakistan that has the potential to bring electricity to rural areas of Pakistan (Andrews, 2006).

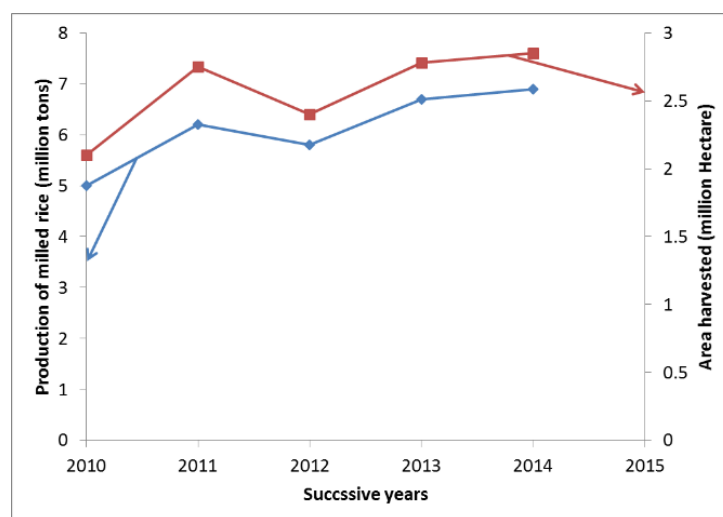


Fig. 1: Production of milled Rice in Pakistan for the successive years (**Indexmundi, 2015**)

This agricultural waste biomass can be used alone or co-fired with coal in the coal power plants for sustainable development of energy, as is done in the UK (Department-of-Energy-and-Climate-Change., 2015). However, such plants are large and expensive and not available for rural energy in Pakistan. The use of 100% biomass plants of the 1 - 10 MW scale are more applicable for rural communities in Pakistan, where there is no national electricity distribution infrastructure.

Biomass is more difficult to mill than coal due to their fibrous structure, whereas coal is a brittle substance that easily fractures in a miller. A further problem with the milling of biomass is that the ash preferentially accumulates in the fine fraction (Saeed et al., 2014). This enrichment of fine particles with inert ash reduces the reactivity of the fine fraction.

A disadvantage of the use of pulverized biomass is that there is an explosion hazard as well as a fire hazard of biomass in storage. Several biomass fire/explosion incidents have occurred with an average rate of one a day (Abbasi and Abbasi, 2007, Eckhoff, 2003). Feeding of biomass into silos with freefall from a conveyor belt feed to the top of the silo also presents an explosion risk due to the generation of fines by particle contact. Some of the recent incidents of biomass fire/explosions are listed in Table 1 (Industrial-Fire-World, 2015). This work addresses the explosion risks for rice husks by measuring the MEC and the K_{st} explosibility index. Also flame propagation rates for pulverized agricultural waste biomass are required for pulverized biomass burner design has had little study and flame speed and burning velocity data is determined in the present work.

Table 1: Recent biomass dust fire/explosion incidents

Date	Type	Plant	Summary
July 17, 2015	Fire + explosion	Bosley Mill Macclessfield, UK	<ul style="list-style-type: none"> ➤ Powerful explosion and fire resulted the collapsing of building. ➤ It led to total 4 causalities and roughly 20 others suffered with minor injuries. ➤ Cause of incident is still under investigation.
April 08, 2015	Fire	Krabi power plant	<ul style="list-style-type: none"> ➤ Two workers injured due to massive fire. ➤ Damage was estimated to be around Bt 100 million.
January 15, 2015	Fire	Docks biomass plant	<ul style="list-style-type: none"> ➤ Woodchip blazed fire in dock plant Southampton, UK. ➤ No injuries were reported.
December 13, 2014	Fire	Gypsum biomass plant	<ul style="list-style-type: none"> ➤ Wood chips on conveyer belt caught fire. ➤ The swift action under covered the fire before it reach to silo storing wood chips. ➤ No injuries and major loss was reported.
November 14, 2013	Fire + explosion	Bay state pellet plant	<ul style="list-style-type: none"> ➤ Fire and explosion originated in the pellet plant, Fitchburg. ➤ No injuries were reported.

2. Characterisation of Rice Husks from Pakistan

Rice husk crop residues (RH) were collected and coarse milled in Pakistan. About 18 kg of rice husk crop residue was prepared in Pakistan and it was fine milled in Leeds to less than 500 μm , using a Retch 100 ultrafine grinder. The fine milled rice husks were sieved into the following size ranges: < 63 μm , 63-150 μm , 150-300 μm , 300-500 μm and < 500 μm . The proportion of the fine fractions collected from sieving was small compared to the coarse fraction, so more milling of the coarse fraction was performed and sieved to get enough fine fraction (<63 μm) for 1 m^3 dust explosion testing, which requires about 1 kg per explosion, for the peak reactivity mixture. The intention in these size fractions was to study rice dust flame propagation where most of the fine fraction had been eliminated and for size ranges say 150 - 300 μm the intention was to eliminate very large and very small particles. However, as will be shown later, each of these sieved samples showed a size distribution over the whole

range so that sieving did not eliminate fines or coarse particles, it simply reduced the proportion. The <500µm sample was investigated as this would have a mixture of fine and coarse particles, so that comparison with say the 300 - 500µm range could isolate the influence of a larger proportion of fines.

Ultimate or elemental analysis of the rice husks was carried out using a Flash 2000 Thermal Scientific Analyser. Two samples of the selected crop residues were tested to show that the composition was uniform. A small amount of each sample was burnt in oxygen in a reactor at around 1800°C. The combustion products were CO₂, H₂O, NO₂ and SO₂ and were separated in a gas chromatographic column prior to individual gas analysis. The oxygen in the sample was determined as the missing mass in the elemental analysis.

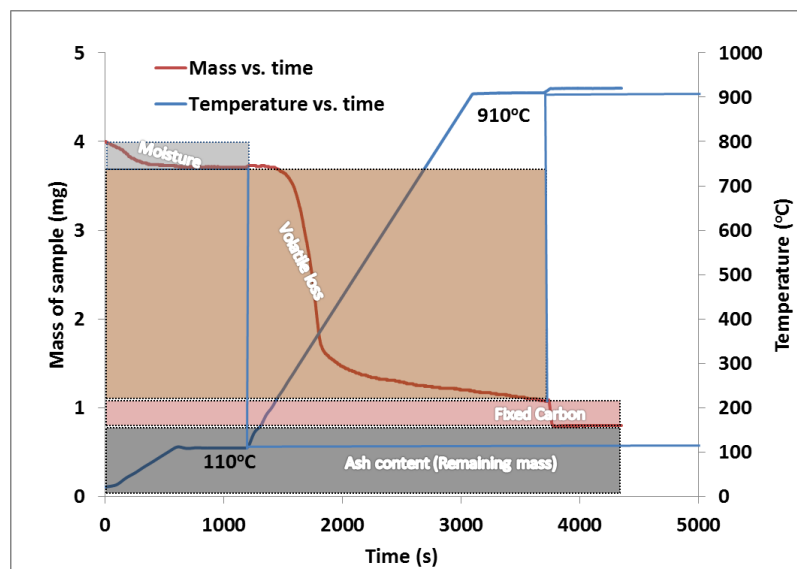


Fig. 2: TGA plot of Rice husk crop residue for proximate analysis

Table 2: Chemical Characterisation of rice husk samples

Ultimate analysis	%C (daf.)	%H (daf.)	%N (daf.)	%S (daf.)	%O (daf.)
Size <500 µm	49.8	6.4	1.1	0.0	42.7
Size <63 µm	48.3	6.8	1.6	0.3	42.5
Proximate analysis	% H ₂ O	% Volatiles	% FC	% ash	
< 500 µm	7.7	62.3	12.2	17.9	
< 63 µm	6.6	51.7	10.5	31.2	
Particle size distribution (Sieve size<63µm)	d (10%)	d (50%)	d (90%)	D ₃₂	D _{4,3}
	13.6	191.6	563.8	33.5	247.7
	CV (MJ/kg)	Bulk density (kg/m ³)	True/Particle density (kg/m ³)	Porosity	
	15.2 Actual 20.4 daf	382	2203	0.83	
Stoichiometric A/F kg/kg	daf A/F	Actual A/F	Actual Conc. g/m ³		
Size <500 µm	6.10	4.53	265		
Size < 63 µm	6.15	3.80	316		

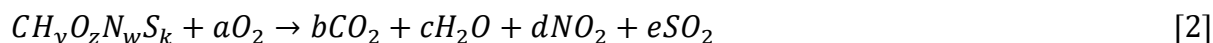
Proximate analysis was performed using a Shimadzu 50 Thermo-gravimetric analyzer. A small mass was weighed, leaving a minimum of 1/3rd of the space in the alumina crucible. This was then placed on a thin wire connected to a sensitive load cell. The mass loss was recorded as a function of temperature in a nitrogen atmosphere up to 910°C. The atmosphere was then changed from nitrogen to air and the fixed carbon was determined by the weight loss. The TGA results for rice husks are shown in Fig. 2. The moisture content was determined with the TGA temperature increased at a rate of 10°C/min and held at 110°C in nitrogen and the weight loss was used to determine the moisture content. The temperature was then increased at 25°C/min to 910°C and held there for 10 minutes to determine the volatile content as the difference in weight between 110°C and 910°C in nitrogen. The nitrogen was switched to air at the same furnace temperature and this burnt out the carbon fraction at 910°C, the remaining residual fraction was ash. The results of the TGA analysis for the different rice husk size fractions are shown in Table 2, together with measurements of the calorific value, bulk density, particle density. The CV_{daf} of biomass was determined from the elemental analysis using the correlation for biomass of Friedl et al. [2005] in Eq. 1.

$$CV_{\text{higher}} = 1.87\%C^2 - 144\%C - 2820\%H + 63.8\%C\%H + 129\%N + 20147 \quad [1]$$

For rice husks the ash fraction was very large, similar to levels in coal. This would act as an inert in the flames and reduce the flame temperature. The calorific value for the overall particle composition was low due to high inert, but was similar to other biomass on a daf basis.

Table 2 shows the composition for two size fractions of the rice husks, > 500 µm and >63 µm. This shows a significant change in composition between the coarse and fine fractions. The N and S are concentrated in the fine fraction as was the ash. This has been found previously by the authors [Saeed et al. 2016a,b] and is thought to be caused by the occurrence of the metal contaminants as fine particles dispersed inside the coarser porous structure of the biomass. This large difference in the ash content gave a considerable difference in the actual stoichiometric A/F with similar values on a dry ash free (daf) basis. The ash fraction can be reduced by water washing the biomass, but this tends to remove compounds other than silica, which form the main part of the ash. The bulk density was almost 6 times lower than the actual particle cell wall density, indicating that there was a large void volume due to the irregular shaped structure of the particles, as shown below in the SEM images.

The stoichiometric air/fuel by mass (A/F) of the rice husk samples were calculated by carbon and oxygen balance using the elemental molar ratios H/C (y) O/C (z), N/C (w) and S/C (k). The stoichiometric molar balance equation is Eq. 2 and the stoichiometric F/A by mass is given by Eq. 3 which gives a stoichiometric A/F of 6.23 for the rice husks, as shown in Table 2.



$$\emptyset=1 \text{ Air/Fuel}_{\text{mass}} = \{[(1+y/4)-z/2-w/4-k/4] 137.94\} / (12+y+16z+14w+32k) \quad [3]$$

The stoichiometric A/F ratio, $\emptyset=1$, for the coarse and fine fractions on a daf basis are converted to the actual concentration accounting for the ash and moisture contents in Table 2. The stoichiometric A/F on a daf basis was very similar for the coarse and fine size fractions, but the large difference in the ash and water content made the actual stoichiometric A/F differ greatly for the fine and coarse fractions.

Sieved fractions of different size ranges were analysed using a Malvern Mastersizer 2000. Table 2 shows the mean particle size for the <63 µm sieved sample was 14, 192 and 564 µm

for 10, 50 and 90% of cumulative volumes respectively. This shows that the 63 µm sieve allowed large particles to pass. This was due to their cylindrical structure, that allow them to pass axially through the sieve holes despite their long lengths. The complete size distributions for the various sieved fractions are shown in Fig. 3. This shows the size distribution for the five sieved size fractions of the milled rice husks.

Fig. 3 shows that all the size fractions by sieving had a wide range of size fractions. Even the 300 – 500 µm sieved fraction had 3% of the mass below 100 µm. The size range for the 63µm sieved size was 2 – 1000 µm, as was that for <500 µm. Thus a wide size distribution is a feature of the milled rice husks. Scanning electron microscopy for raw <500 µm rice husk samples are shown in Fig. 4a. This shows that very wide range of sizes from small spheres to long thin splinters of rice husks. Fig. 4 shows that there were many long thin cylinders in the

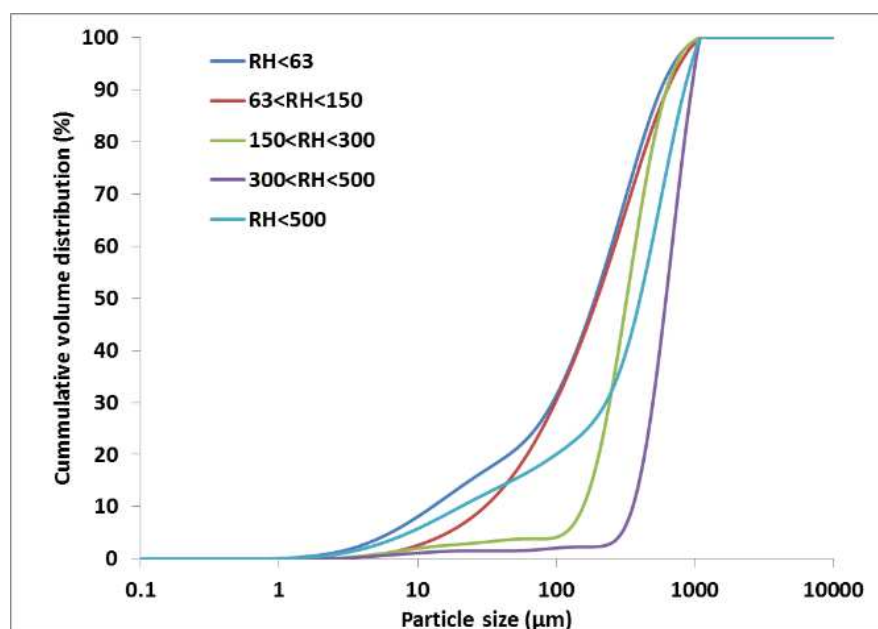
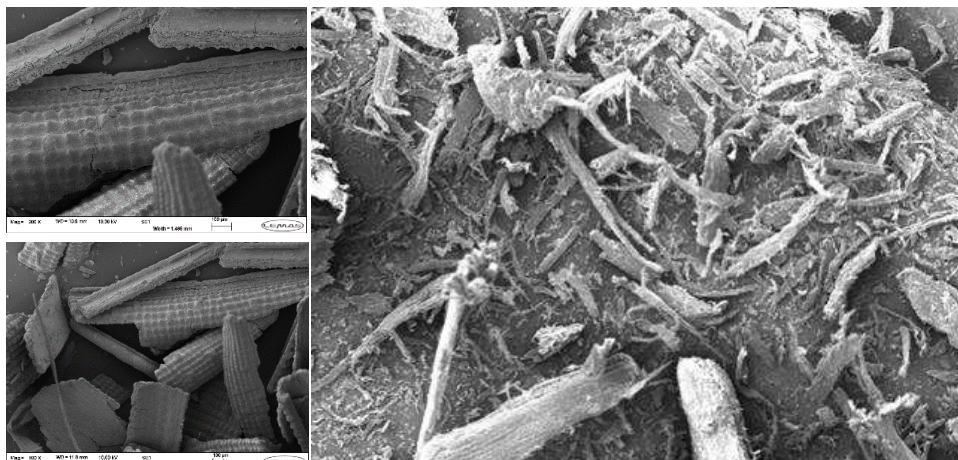
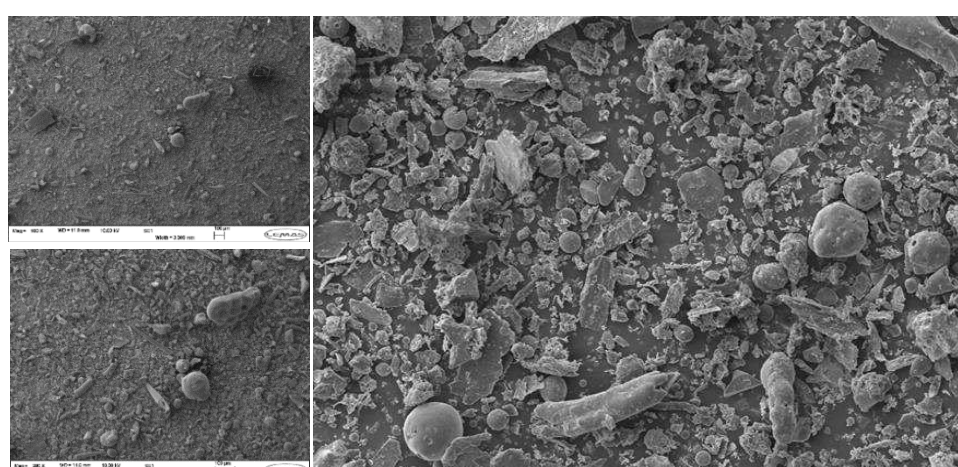


Fig. 3: Particle size distribution of different size range fractions of Rice husk (RH)



(a) Raw Rice husk



(b) Post explosion residue

Fig. 4: Scanning Electron Microscopy of Rice husk and its post explosion residue

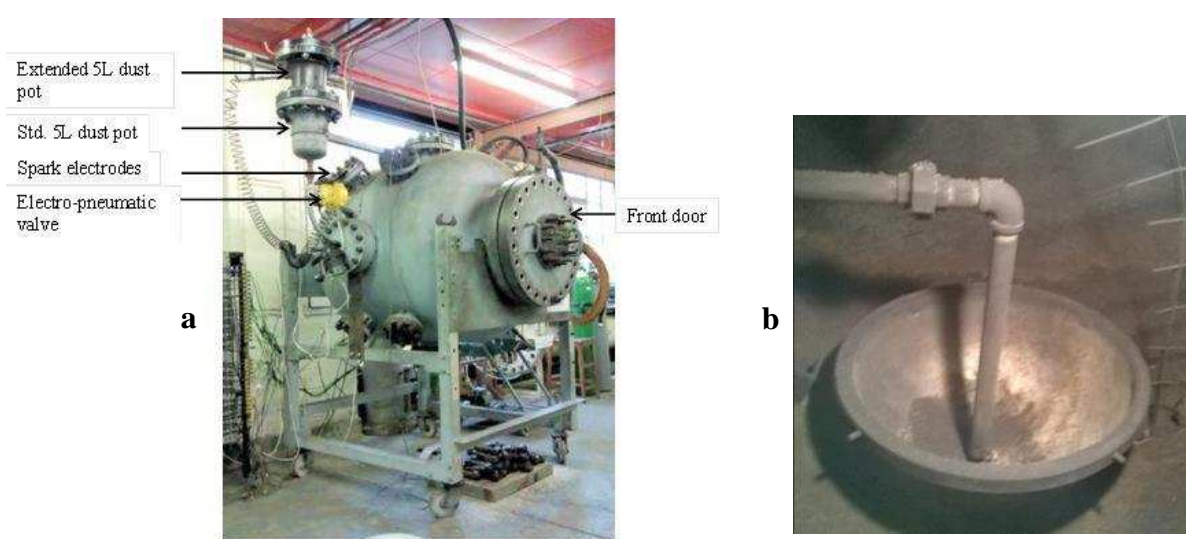


Fig. 5: a) Modified 1 m³ vessel b) Hemispherical disperser

sample and these under agitation would pass through a sieve with size similar to the diameter of the long cylinders. These were then identified by the laser scatter size analyser as large particles in Fig. 3.

3. Experimental Methods

Fig. 5 shows the ISO 1m³ vessel along with the hemispherical disperser for determining the flame speed and explosion properties of rice husks for a range of particle sizes in Fig. 3. The 1 m³ vessel design followed the guidance in the ISO standard (ISO 6184-1, 1985). Piezo resistive pressure transducers were fitted to the external dust and compressed air injection vessel and the main explosion vessel volume. The pressure was recorded as a function of time in the explosion using a 32 channel Microlink data acquisition system with 100 kHz data acquisition rates per channel. The peak explosion pressure and the maximum rates of pressure rise was determined and from these records the deflagration rate, K_{st}, was determined, as in Eq. 4.

$$K_{st} = (dp/dt)_{max} V^{1/3} \text{ bar m/s} \quad (4)$$

The vessel was instrumented to enable the flame speed to be measured (Sattar et al., 2012b, Sattar et al., 2012a, Saeed et al., 2015a, Phylaktou et al., 2010). A vertical and horizontal array of bare bead thermocouples were placed at known interval in the constant pressure period of the explosion. The output of the thermocouples were recorded on the 32 channel Microsoft data acquisition system and the time of flame arrival at each thermocouple was determined from the thermocouple output records as a sudden increase in output current as the flame arrived at the thermocouple. The aim was not to measure the temperature but the time of flame arrival, so that the accuracy of temperature measurement was not important. This time of flame arrival was plotted as a function of the thermocouple position for the two thermocouple arrays. If a spherical flame was propagating then the two lines would be in agreement and this was the case in all the experiments report here. To achieve the spherical flame propagation, which has rarely been demonstrated in dust explosions, the 10 kJ chemical ignitor was constructed of two 5 kJ ignitors that impinged on a hemisphere to produce a central ball of flame, instead of the more usual ignitor linear flame jet ignition which was found not to produce a spherical flame. The K_{st} measurement in Eq. 4 is based on the assumption of spherical flame propagation and if this is not achieved then the K_{st} measurement is in error. The repeatability of the K_{st} measurements was +/- 8%.

The standard ISO 1m³ dust explosion vessel has a 5 L external dust injection vessel where the dust for the explosion is placed and pressurized to 20 bar with air for dust injection at the start of the explosion. The ignition occurs 0.6s after the start of arrival of the dust into the test vessel, determined by the increase in pressure of the vessel. However, this system in the experience of the authors does not work with coarse biomass. There are two problems that the authors have found solutions to: the low bulk density of pulverized biomass makes the 5L capacity of the external vessel too small to hold the 1kg or more of biomass that is required in the tests. A 10L external vessel was used at 10 bar injection pressure, so that the total mass of external air was the same. This was calibrated on the ignition delay to give the same K_{st} for cornflour as in the reference method (Satter, H., 2013). However, for biomass that was filtered to <63μm the size distribution for woody or agricultural biomass, as shown in Fig. 3, still had large particles present and these resulted in the C ring delivery tube blocking, so that these types of biomass could not be tested. The standard C ring dust injection mode was good for nut type brittle biomass but not for fibrous biomass (Satter, H., 2012a).

In the present work relatively coarse rice husks would not operate with the standard injection system and a new injection system was designed that placed all the biomass inside the

explosion vessel at the start of the test and dispersed it with the external compressed air source using an injection pipe located close to the bottom of a hemispherical container, 0.4m diameter, as shown in Fig. 5b. This was developed after several unsuccessful attempts at alternative methods of dispersing the dust internally. The principle is the same as that used successfully for many years in the Hartmann equipment, which places the dust inside the explosion vessel (vertical tube) and then disperses it with external compressed air. The hemispherical disperser air injection pipe had holes drilled in the end part, that were immersed in the dust to be dispersed. These were the same diameter and number as for the standard C ring and this ensured the same rate of delivery of air. This hemispherical dispersion system was calibrated using cornflour and compared to the standard C ring disperser. The optimum ignition delay was calibrated to be 0.5s. The turbulence factor was determined to be 4.7, using 10% methane-air explosions with and without compressed air injection. This was comparable to the turbulence factor determined for the standard C ring disperser. The measured turbulent flame speed, S_T , was converted into a laminar flame speed, S_L , by dividing by the 4.7 turbulent to laminar flame speed ratio. The laminar burning velocity, S_u or U_L , of the dust was then determined as S_L/E where E is the expansion ratio which is taken as the same as the measured P_m/P_i (Cashdollar, 1996).

A feature of dust explosions in the ISO 1m³ dust explosion equipment is that about half of the dust injected does not participate in the explosion and is left on the bottom of the vessel at the end of the test. This changes the mass of dust that participated in the explosion and the mass that did not burn was collected and weighed and the mass that burnt was determined. This also changed the effective equivalence ratio of the combustion and the results are reported in terms of the corrected or burnt equivalence ratio. The analysis of this residue is discussed in detail later, where it is shown to have a finer particle size distribution for the whole <500μm size range. An SEM of the residue is also shown in Fig. 4b where a lower proportion of the long cylindrical particles can be seen. Fig. 4b also shows that there was some thermal action on the particles as there are round spheres of molten ash present, which are quite different in appearance to the rest of the particles. The origin of this unburnt mass dust at the end of the test was due to the action of the explosion induced wind ahead of the flame front on the array of coarse particles. The overall action was to entrain the particles ahead of the flame and blow them onto the vessel wall. A layer of unburnt particles collected there and the flame impinged on the outer layer and caused partial pyrolysis. Once the pressure reduced after the explosion as the gases cooled, the particles on the wall fell off to form a heap of particles on the floor of the chamber. For some particles such as milk powder and sugar the particles remain attached to the wall as a thin skin, but this did not occur in the present work.

The equivalence ratio of the mixture that the flame propagated in was that based on the mass of fuel burnt, which was the difference in the initial mass placed in the hemisphere inside the vessel and the residual mass collected from the bottom of the explosion vessel after the test. This was expressed as a burnt air to fuel ratio, A/F, by mass using the total mass of air in the vessel and that injected. The stoichiometric A/F was determined by carbon balance from the rice husk composition, as in Table 2 for the actual composition of the rice husks including the ash and water. The ratio of the stoichiometric to explosion burnt gas A/F was the explosion burnt equivalence ratio and the results are presented as a function of the burnt gas equivalence ratio.

4. Results and discussion

4.1 Reactivity of raw crop residues

The reactivity of pulverized rice husk crop residues for different size fractions were investigated and the minimum explosive concentration (MEC) was determined together with the K_{st} and burning velocities as function of the burnt gas equivalence ratio, ϕ . The range of ϕ investigated was limited due to the limited quantity of milled rice husk that was available. However, sufficient ϕ were investigated to determine the peak P_{st} and burning velocities and the ϕ at which this maximum reactivity occurred.

4.1.1 Peak pressure

The maximum explosion pressure in each explosion, normalized to the initial ambient pressure, is shown as a function of the burnt equivalence ratio in Fig. 6. The maximum pressure ratio was relatively independent of the particle size and was in the range 7.3-7.45. This indicates that the completeness of combustion was similar irrespective of the particle size. This is as expected, as the peak pressure is controlled by the peak flame temperature and this is not dependent on the particle size but is controlled by the mass of biomass consumed in the flame front or its equivalence ratio. Table 3 compares the present results with those of the authors for other biomass and this shows that P_m/P_i varies between 7.3 and 9.4 which shows that the present results are the lowest of all the biomass in Table 3. The highest P_m/P_i was for nut shell biomass. The reason for the low P_m/P_i for the present rice husks was the high ash content, especially as after milling it was concentrated in the fine fraction at 31% of the mass. This effectively reduced the calorific value of the biomass as the inert material acts as a heat sink. This resulted in lower flame temperatures and hence low P_m/P_i . For rice husks to be a practical biomass fuel the ash would have to be reduced by a combination of water and acid washing. However, rice husks are in plentiful supply around the world as well as in Pakistan and it is worthwhile to make it into a practical biomass fuel. In terms of an explosion risk it is clear that even with 31% ash in the fine rice husks there is still a significant explosion hazard in the dust associated with processing and storage of rice husks. A coarse particle explosion will cause just as much damage to plant as a fine particles explosion as this is controlled by the pressure rise.

The two particle size ranges 150-300 μm and 300-500 μm did not propagate a flame from the 10 kJ chemical ignitor. The particle size distribution in Fig. 3 showed that these two particle size ranges had <5% fines and this was critical to their lack of ability to propagate a flame. Similar work to the present was carried out by Saeed et al. (2017) on a thermally processed pine wood sample, as summarized in Table 3. This had explosions for the all the size ranges that exploded in the present work, but also for 150-300 μm , but not for 300-500 μm . The

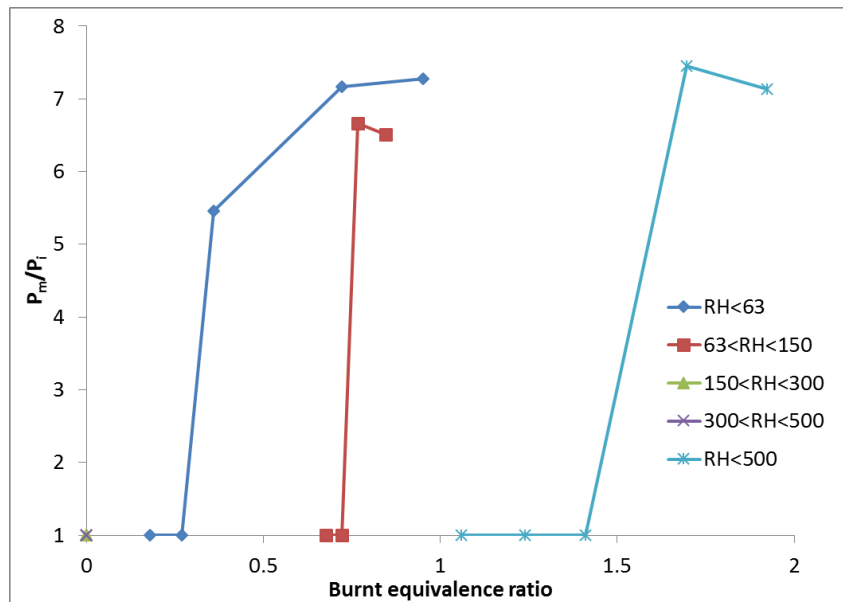


Fig. 6: P_m/P_i vs. burnt equivalence ratio for different sized fractions of rice husk (RH)

reason that the 150–300 μm size range exploded in this mixed wood sample was that the size distribution had a greater proportion of fines at 20% compared with 5% in Fig. 3.

A key feature of Fig. 6 was that the burnt equivalence ratio at which the peak pressure occurred was much richer for the <500 μm particle size than <63 μm , as summarized in Table 3. It is likely that the rather lean mixture for the peak pressure for the 63 – 150 μm size range was because an inadequate range of mixture concentrations had been tested, due to the lack of sieved mass. Previous work of the authors (Saeed et al., 2017) for a thermally processed pine wood, which is summarised in Table 3, showed a similar richer mixture for the peak pressure for coarse particle sizes. The reason for the rich mixtures for coarse particle sizes is that the coarse mixtures propagate in the fine particles blown ahead of the flame and that the larger particles in the coarse size fraction burn in the products of combustion of the fines. This would mean that sufficient fines were required to achieve a flammable mixture and to achieve this, the overall mixture was much richer than for propagation in the fines only.

4.1.2 Deflagration index vs. burnt equivalence ratio

Fig. 7 shows the deflagration index, K_{st} , as a function of the burnt equivalence ratio for three size fractions of selected rice husk residues. The size fraction with a higher proportion of fines had a higher K_{st} , showing as expected that fine particles were more reactive. The peak values of K_{st} were a strong function of the particle size, as summarized in Table 3, with 82 bar m/s for the rice husks <63 μm and 35 bar m/s for the larger size fractions. The reduced K_{st} for the larger size fractions was due to the mechanism of flame propagation for large size fractions, with the flame propagating in the fines ahead of the flame and the larger particles burning in the products of combustion. The fines ahead of the flame would burn hotter as they were locally nearer stoichiometric and the increase in equivalence ratio as the coarse material burnt behind the flame front would slow the flame front down as the temperature would be reduced. Also for the richer mixtures involved in coarse particle size flame propagation there was a larger fraction of ash which acted as a heat sink and this reduced the reactivity.

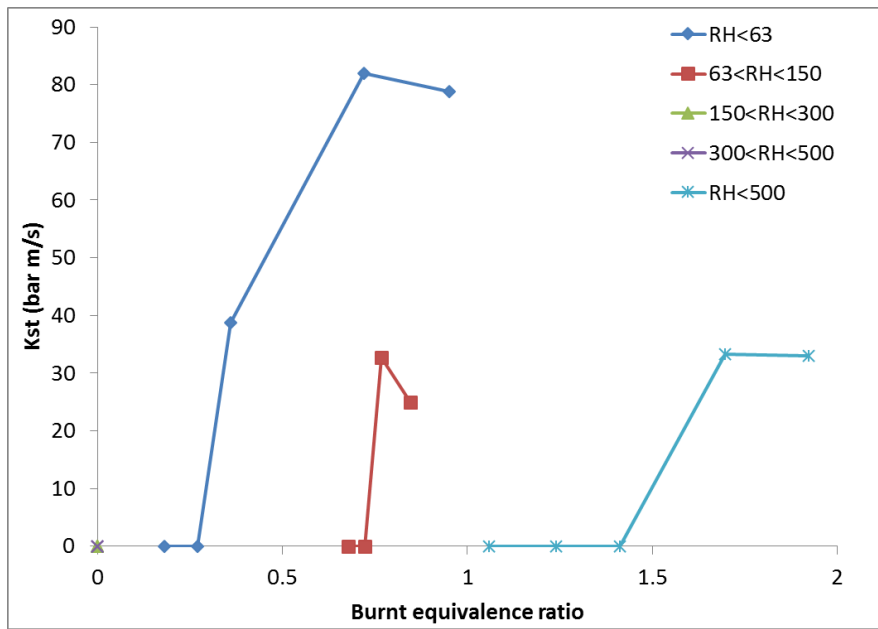


Fig. 7: K_{st} vs. burnt equivalence ratio for different sized fractions of rice husk (RH)

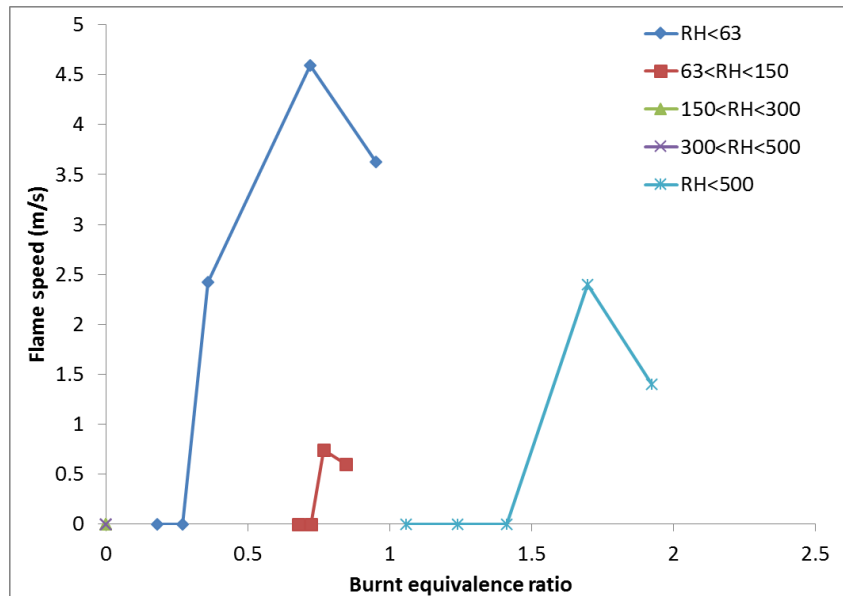


Fig. 8: P_m/P_i vs. burnt equivalence ratio for peanut shell and corn cobs in comparison to coals

For the fine fraction $< 63\mu\text{m}$ the K_{st} for other biomass, investigated on the same equipment, is summarized in Table 3 and was from 120 bar m/s for the steam exploded pine to 81 for spruce wood. The rice husk are at the bottom of this range at 82 bar m/s and this was due to the lower flame temperature, indicated by the low P_m/P_i . Also, the large ash fraction of the fine fraction also reduced the reactivity. For the more reactive mixtures the size fraction $< 63 \mu\text{m}$ was finer for the more reactive mixtures. For the coarse fraction $< 500\mu\text{m}$ Table 3 shows that the range of K_{st} was from 24 to 60 bar m/s and the present work on rice husks with 35 bar m/s was more reactive than would be expected from the $< 63 \mu\text{m}$ results. Part of the reason for this was that the ash fraction of the coarse particles was reduced relative to the fine fraction as shown in Table 2. All the coarse fractions $< 500\mu\text{m}$ in Table 3 showed a much reduced K_{st} , relative to

Table 3 Comparison of the present results with those for other biomass

Samples	ϕ_{peak} K_{st}	Peak P_m/P_o	Peak K_{st} bar m/s	Peak S_T m/s	Peak S_u m/s	Refs.
Rice husks <63	1.0	7.3	82	4.6	0.13	This work
Rice husks <500	1.7	7.5	35	2.5	0.07	This work
Rice husks 63-150	0.9	6.7	35	0.8	0.03	This work
Corn cob<500μm	1.8	8.0	60	1.3	0.03	(Saeed, 2016c)
Peanut Shells <500μm	2.7	7.1	25	1.3	0.04	(Saeed, 2016c)
Steam Exploded Pine <63μm	2.1	8.6	120	5.4	0.13	(Saeed, 2017)
Steam Exploded Pine 63-150μm	1.7	7.2	50	2.0	0.06	(Saeed, 2017)
Steam Exploded Pine 150-300μm	3.0	7.0	45	1.3	0.04	(Saeed, 2017)
Steam Exploded Wood SPF<500μm	3.3	7.3	24	1.05	0.03	(Saeed, 2016d)
Bagasse<63μm	2.7	8.8	103	3.8	0.11	(Saeed 2015c)
Wheat	1.6	8.5	82	3.0	0.13	(Saeed, 2015c)
Straw<63μm	2.4	9.3	82	3.7	0.27	(Sattar 2012a)
Pistachio nut shells<63μm	2.8	9.4	98	5.1	0.24	(Sattar 2012a)
Walnut shells<63μm	4.2	9.0	109	3.7	0.1	(Huéscar Medina 2013)
Pine 1<63μm	1.9	8.8	81	3.4	0.09	(Huéscar Medina 2014b)
US Pine 2<63μm	2.5	9.0	105	4.5	0.11	(Huéscar Medina 2014a)

the <63 μm results, but the P_m/P_i were very similar. This indicates that for both size fraction combustion was complete. The mechanism of combustion of the coarse fraction was for the leading flame to be burning a fine fraction blown ahead of the flame by the explosion induced wind. However, this would burn as soon as it was in the flammable range and would not be stoichiometric which would give fast flames.

4.1.3 Turbulent flame speed vs. burnt equivalence ratio

The turbulent flame speeds for rice husks are shown as a function of equivalence ratio in Fig. 8 for the three size fractions that propagated a flame. The fine fraction <63 μm had a peak turbulent flame speed of 4.6 m/s whereas the size fraction with less fines showed lower flame speeds 2.5 m/s for the <500μm sample and 0.8 m/s for the 63 - 150μm sample. A comparison with other biomass turbulent flame speeds is shown in Table 3 and the range of turbulent flames speeds for particles <63 μm was 5.4 – 3.0 m/s and the present results were one of the highest flame propagation speeds. For coarse particles <500 μm the turbulent flame speed range was from 1.05 to 2.5 m/s and the present rice husk results were the highest of the four biomass with <500 μm coarse size. Fig. 3 shows that 20% of the <500 μm size range for rice husks was <100 μm and this will control the flame propagation. For particles with lower

turbulent burning velocity the size range of the particles had less than the 20% of fines in the present work.

4.2 Analysis of rice husk post explosion residues

4.2.1 Ultimate and proximate analysis of post explosion residues

Table 4 shows the ultimate and TGA analysis of the post explosion residues for the most reactive concentration of different sized fractions. Elemental analysis showed almost same composition for all the size fractions as that of raw sample. However the TGA analysis of the explosion residues showed reduced volatile content relative to the raw biomass. The volatiles in the explosion residues were higher for the fine fraction in comparison to coarse. This was because there was more release of volatiles from the fines due to their more exposed surfaces. The ash content was increased in the post explosion residues as expected, as they contained the ash from the burnt rice husks as well as the ash from the unburnt rice husks. Stoichiometric air to fuel ratios were calculated for the residues to be almost the same as the raw biomass, on a dry ash free basis. This indicated little compositional change of the particles apart from the increase in the ash content.

Table 4: Chemical characterization of the post explosion residues in comparison to raw rice husk

Biomass	Raw rice husk	Post explosion Rice husk (RH) residues		
		RH<63µm	RH(63-150µm)	RH<500µm
% C (daf.)	49.8	50.2	49.9	51.2
% H (daf.)	6.4	6.6	6.4	5.7
% N (daf.)	1.1	1.5	0.7	0.6
% S (daf.)	0.0	0.0	0.0	0.0
% O (daf.)	42.7	41.7	43.0	42.5
% H ₂ O	7.7	4.8	5.8	5.6
% VM	62.3	39.9	57.5	61.3
% FC	12.2	10.8	14.3	8.0
% Ash	17.9	44.6	22.3	25.2
CV (MJ/kg)	15.2	13.9	15.6	15.7
Stoich. A/F (g/g) daf	6.1	6.3	6.1	6
Actual stoich. conc. (g/m ³)	262.3	376.4	273.6	289.0

4.2.2 Particle size distribution

The particle size distribution of the residues after the explosion were determined in the same way as for the raw biomass. Cumulative plots of the particle size distribution showed the increase in size for the fine fraction. This was due to the formation of large fused ash layers in the sample, as shown in the SEM analysis in Fig. 4b. However, for the coarse fractions the trend was different as the size fraction 63-150 µm showed an increase in the size of the post explosion residue for 10% cumulative volume, but almost same for 50 and 90% of the cumulative volume. The coarse fraction <500 µm contained the least fines and showed the reverse trend with a reduction in size in the residue, as shown in Fig. 9. This was due to the

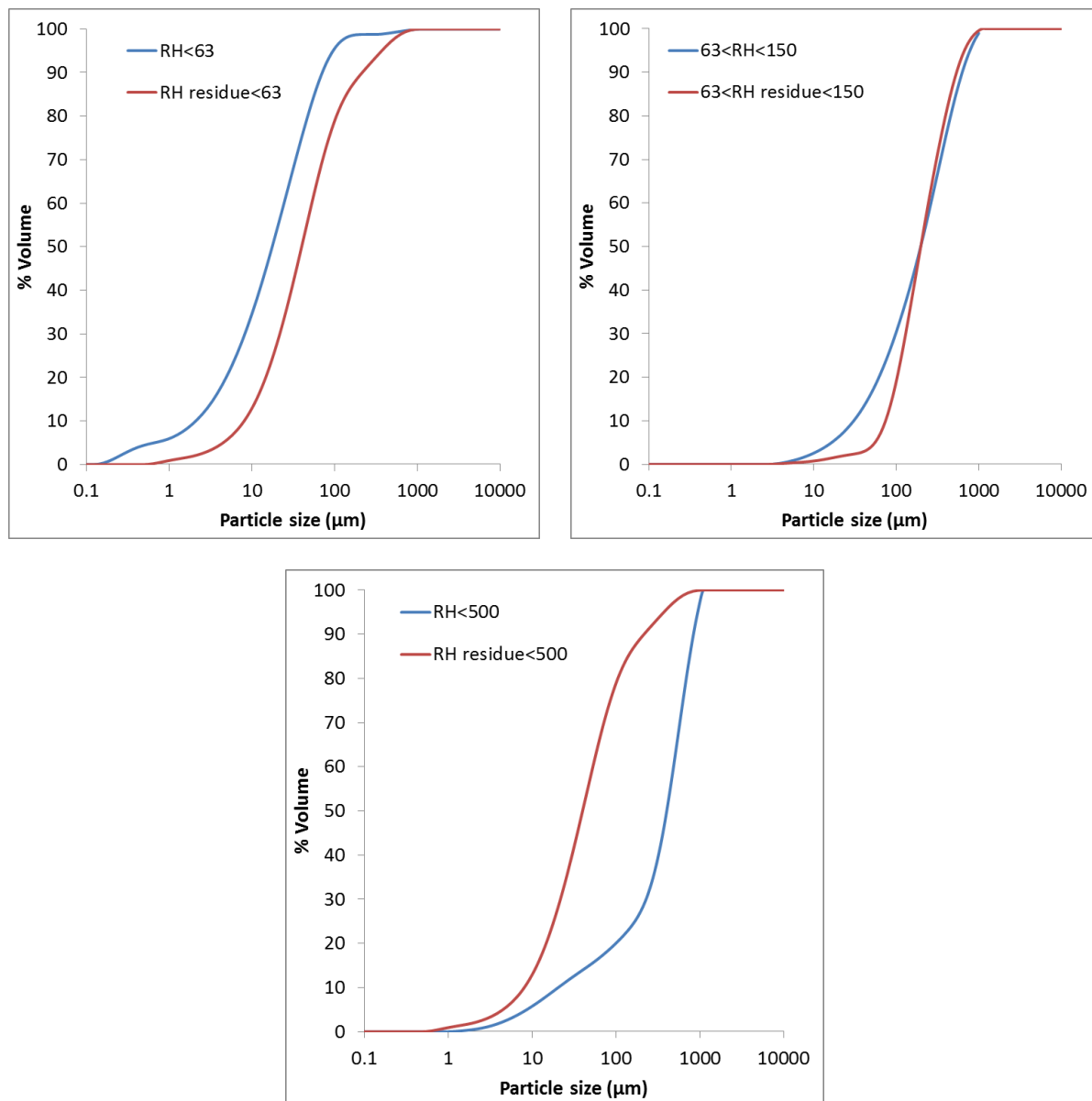


Fig. 9: Cumulative analysis of different sized fractions of rice husk in comparison to respective post explosion residues

partial burning of coarse particles leaving smaller sizes after the flame propagation. The size fraction 63-150 μm showed an increase in the size of the post explosion residue for 10% cumulative volume, but almost the same for 50 and 90% of the cumulative volume. The coarse fraction <500 μm contained the least fines and showed the reverse trend with a reduction in size in the residue, as shown in Fig. 9. This was due to the partial burning of coarse particles leaving small sizes after the flame propagation..

4.2.3 Surface morphological study

Scanning electron microscopy was performed as shown in Fig. 4a on the rice husk and Fig. 4b for the post explosion residues. Samples of raw rice husks was observed to have a wide variation in particle sizes and shape. Also the particles were observed to be thin tubes that resulted in the efficient release of volatile. It was found that the post explosion residue for <63

μm sample had molten ash with the formation of cenospheres indicating higher siliceous minerals in the ash contents.

4.3 Comparison of modified ISO 1 m³ and previous Hartmann results (Saeed et al., 2014)

The MEC of rice husks were presented as a function of the average particle sizes for different size range fractions in Fig. 10. The fine fraction MEC was slightly lower in the current study using the 1m³ dust explosion vessel measurements in comparison with the Hartmann results. However, for coarser fractions the trend was the opposite to that for the 1m³ results. This difference may not be significant, as both methods of measuring the MEC have uncertainties. In the Hartmann equipment the dust may not be fully dispersed and mixed with the air. For the ISO 1 m³ results, the burnt gas equivalence ratio measurement procedure has errors in the determination of the mass of unburnt residue. However, it was still believed that the Hartmann equipment was a more suitable measurement method for the measurements of minimum explosive concentration, as the problem of a large fraction of the dust mixture not burning in the ISO 1 m³ method, meant that the corrections to the nominal equivalence ratio were large.

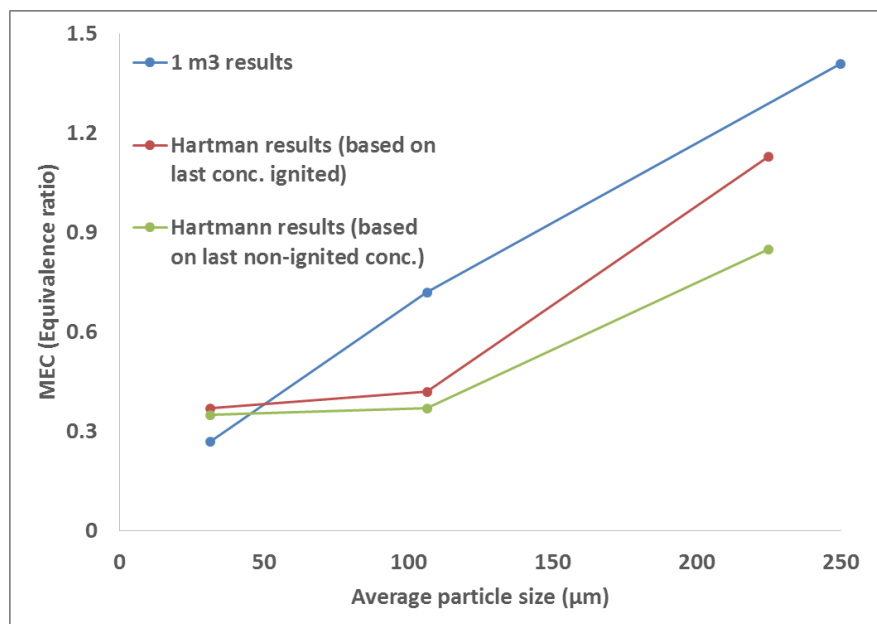


Fig. 10: MEC comparison of different size fractions rice husk using modified 1 m³ and Hartmann measurements

5. Conclusions

Different size fractions of rice husk were tested using a modified ISO 1m³ vessel with a hemispherical disperser. This new disperser was calibrated for the ignition delay using cornflour to give the same K_{so}. The objective was to study the flame propagation behavior of fine and coarse size range fractions of rice husk dusts. Size distribution with 150 - 300 μm and 300 - 500 μm would not explode and it is clear that some fines are necessary for coarse particles to explode. The results showed a P_m/P_i of 8.2 for <63 μm and 8.3 for <500 μm and this showed that coarse particles had an explosion risk that involved the same physical damage by overpressure as fine particles. There were larger differences in K_{st} and U_T between the fine and coarse size fractions. The K_{st} was 82 for <63 μm and 35 for <500 μm . The MEC

was similar between the ISO 1 m³ and the Hartmann explosion tube and for <63µm was 0.30 for both techniques. The large inert content of rice husk dusts made the dust less reactive than for other dusts with lower ash content. The propagation of coarse particles was due to the flame propagation occurring in the fines ahead of the main flame, entrained by the explosion induced wind. The coarse particles then burnt in the products of combustion of the fines ahead of the flame.

The explosion had a residue that was a significant proportion of the mass of particles injected and the equivalence ratio at the flame front was corrected for the particle mass loss. The analysis of the residue showed that the composition was the same as the original rice husks, apart from the increase in the ash fraction, which contained the ash from the burnt particles. Rice husk can be employed as a practical fuel with less milling required due to their ability to propagate the flame for coarse size ranges.

Acknowledgements

The authors gratefully acknowledge the financial support of 'Faculty Development Program' from University of Engineering and Technology, Lahore, Pakistan.

References

- Abbasi, T. & Abbasi, S. (2007). Dust explosions—Cases, causes, consequences, and control. *Journal of Hazardous Materials*, 140: 7-44.
- Amjid, S. S., Bilal, M. Q., Nazir, M. S. & Hussain, A. (2011). Biogas, renewable energy resource for Pakistan. *Renewable and Sustainable Energy Reviews*, 15: 2833-2837.
- Andrews, G. E. & Phylaktou, H. N. (2010). *Explosion Safety. Handbook of Combustion*. Edition type ed.: John Wiley and Sons, Inc.
- Andrews, S. S. (2006). Crop residue removal for biomass energy production: Effects on soils and recommendations. US Department of Agriculture—Natural Resource Conservation Service, http://soils.usda.gov/sqi/files/AgForum_Residue_White_Paper.pdf (15 November 2012).
- Asia-Rice-News. (2015). Riceoutlook [Online]. Available: <http://www.riceoutlook.com/category/rice-updates/asia-rice-news/pakistan-rice-news/> [Accessed 23 November 2015].
- K. L. Cashdollar, (1996). Coal dust explosibility. *Journal of loss prevention in the process industries*, 9(1): page 65-76.
- Department-of-Energy-and-Climate-Change. (2015). Digest of United Kingdom Energy Statistics (DUKES), UK.
- Dorosh, P. & Thurlow, J. (2015). *Agriculture Productivity Growth and Rural Welfare: Insights from Economy-wide Analysis*.
- Eckhoff, R. K. (2003). *Dust Explosions in the Process Industries: Identification, Assessment and Control of Dust Hazards*. Gulf Professional Publishing, Amsterdam. 3rd ed.
- Friedl, A., Padouvas, E., Rotter, H. Vermuza, K, Prediction of heating values of biomass fuel from elemental composition, *Anal Chim Acta*, 544 (2005) 191-198.
- Indexmundi. (2015). Factbook [Online]. Available: <http://www.indexmundi.com/pakistan/> [Accessed 1st April 2015].
- Industrial-Fire-World. (2015). Incident logs [Online]. Available: <https://fireworld.com/IncidentLogs.aspx> [Accessed 10 November 2015].

- ISO 6184-1 (1985). Explosion Protection Systems. Part 1: Method for determination of Explosion Indices of Combustible Dusts in Air.
- Phylaktou, H., Gardner, C. & Andrews, G. (2010). Flame speed measurements in dust explosions. Proceedings of the Sixth International Seminar on Fire and Explosion Hazards. 695-706.
- Saeed, M. A., Medina, C. H., Andrews, G. E., Phylaktou, H. N., Slatter, D. & Gibbs, B. M. (2014). Agricultural waste pulverised biomass: MEC and flame speeds. Journal of Loss Prevention in the Process Industries, 36: 308-317.
- Saeed, M. A., Andrews, G. E., Phylaktou, H. N., Slatter, D. J. F., Medina, C. H. & Gibbs, B. M. (2015a). Flame Propagation of Pulverised Biomass Crop Residues and their Explosion Characteristics 25th International Colloquium on the Dynamics of Explosions and Reactive Systems (ICDERS), Leeds, UK.
- Saeed, M. A., Irshad, A., Sattar, H., Andrews, G. E., Phylaktou, H. N. & Gibbs, B. M. (2015b). Agricultural Waste Biomass Energy Potential in Pakistan. Proc. International Bioenergy Exhibition and Asian Bioenergy Conference, Shanghai.
- Saeed, M.A., Slatter, D.J.F. Andrews, G.E., Phylaktou, H.N. and Gibbs, B.M. (2016a) Combustion of Pulverized Biomass Crop Residues and Their Explosion Characteristics. Combustion Science and Technology Vol. 188 , Issue 11-12, Pages 2200-2216, <http://DX.DOI.ORG/10.1080/00102202.2016.1212604>
- Saeed M.A, Slatter D.M., Andrews G., Phylaktou H., Gibbs B., (2016b), The burning velocity of pulverised biomass: the influence of particle size, Chemical Engineering Transactions, 53, 31-36 DOI: 10.3303/CET1653006
- Saeed, M.A., Slatter, D.J.F., Andrews, G.E., Phylaktou, H.N. and Gibbs, B.M. (2016c). Flame Speed and K_{st} Reactivity Data for Pulverised Corn Cobs and Peanut Shells. Proceedings of the 11th International Symposium on Hazards, Prevention and Mitigation of Industrial Explosions, 11th ISHPMIE, Dalian, China. p.422-434.
- Saeed M.A, Slatter, D.J.F., Andrews G.E., Phylaktou H.N. & Gibbs B.M., Walton, R.and Lucasz Niedzweicki. (2016d). Explosions and Flame Propagation of Coarse Wood: Raw and Torrified. Proc. 8th International Seminar on Fire and Explosion Hazards, Hefei, China, April 25 – 29, 2016. 10pp. Editors: J. Chao, V. Molkov, P. Sunderland, F. Tamanini, J. Torero, USTC Press.
- Saeed, M.A., Anez, N.F., Andrews, G.E., Phylaktou, H.N. and Gibbs, B.M. (2017) Steam exploded pine wood burning properties with particle size dependence, Fuel. ISSN 0016-2361, Fuel, Volume 194, 15 April 2017, Pages 527-532
- Sattar, H., Phylaktou, H. N., Andrews, G. E. & Gibbs, B. M. (2012a). Explosions and Flame Propagation in Nut-shell Biomass Powders. Proc. of the IX International Seminar on Hazardous Process Materials and Industrial Explosions (IX ISHPMIE), Cracow.
- Sattar, H., Slatter, D. J. F., Andrews, G. E., Gibbs, B. M. & Phylaktou, H. N. (2012b). Pulverised Biomass Explosions: Investigation of the Ultra Rich Mixtures that give Peak Reactivity. Proc. of the IX International Seminar on Hazardous Process Materials and Industrial Explosions (IX ISHPMIE), Cracow.
- Sattar H., Huescar, C.M., Phylaktou, H.N., Andrews, G.E. and Gibbs, B.M., (2013). Calibration of a 10L Volume Dust Holding Pot for the 1 m³ Standard Vessel for Use in Low Bulk Density Biomass Explosibility Testing. Proceedings of the Seventh International Seminar on Fire and Explosion Hazards (ISFEH7), pp.791-800. Research Publishing. doi:10.3850/978-981-07-5936-0_13-02.

